Differential Trafficking and Timed Localization of Two Chitin Synthase Proteins, Chs2p and Chs3p

John S. Chuang and Randy W. Schekman

Department of Molecular and Cell Biology, and Howard Hughes Medical Institute, University of California, Berkeley 94720

Abstract. The deposition of the polysaccharide chitin in the *Saccharomyces cerevisiae* cell wall is temporally and spatially regulated. Chitin synthase III (Chs3p) synthesizes a ring of chitin at the onset of bud emergence, marking the base of the incipient bud. At the end of mitosis, chitin synthase II (Chs2p) deposits a disk of chitin in the mother-bud neck, forming the primary division septum. Using indirect immunofluorescence microscopy, we have found that these two integral membrane proteins localize to the mother-bud neck at distinct times during the cell cycle. Chs2p is found at the neck at the end of mitosis, whereas Chs3p localizes to a ring on the surface of cells about to undergo bud emergence and in the mother-bud neck of small-budded cells. Cell synchronization and pulse-chase experiments suggest that the timing of Chs2p localization results from cell cycle–specific synthesis coupled to rapid degradation. Chs2p degradation depends on the vacuolar protease encoded by *PEP4*, indicating that Chs2p is destroyed in the vacuole. Temperature-sensitive mutations that block either the late secretory pathway (*sec1-1*) or the internalization step of endocytosis (*end4-1*) also prevent Chs2p degradation. In contrast, Chs3p is synthesized constitutively and is metabolically stable, indicating that Chs2p and Chs3p are subject to different modes of regulation. Differential centrifugation experiments show that a significant proportion of Chs3p resides in an internal compartment that may correspond to a vesicular species called the chitosome (Leal-Morales, C.A., C.E. Bracker, and S. Bartnicki-Garcia. 1988. *Proc. Natl. Acad. Sci. USA.* 85:8516–8520; Flores Martinez, A., and J. Schwencke. 1988. *Biochim. Biophys. Acta.* 946:328–336). Fractionation of membranes prepared from mutants defective in internalization (*end3-1* and *end4-1*) indicate that the Chs3p-containing vesicles are endocytically derived. Collectively, these data suggest that the trafficking of Chs2p and Chs3p diverges after endocytosis; Chs3p is not delivered to the vacuole, but instead may be recycled.

THE polysaccharide chitin is deposited into the cell wall of *Saccharomyces cerevisiae* in a spatially and temporally regulated manner (for review see Cabib et al., 1982; Bulawa, 1993; Cid et al., 1995). In contrast with the major cell wall polysaccharides, glucans and mannans, which are found over the entire cell surface, chitin is specifically localized. A chitin ring forms on the cell surface in late G1, before bud emergence. This annulus predicts the site of bud emergence and persists at the junction between the mother and the growing bud. At the end of mitosis, centripetal synthesis within the chitin ring results in the formation of a disk of chitin called the primary division septum. This event initiates the process of cell separation. Secondary septa, comprised of glucans and mannans, are subsequently laid down on each side of the primary division septum. Finally, cell separation is effected by the action of an endochitinase, which partially hydrolyzes the chitin septum, resulting in the physical separation of the mother and the daughter cell. The localized deposition of chitin during specific points in the cell cycle has been of interest as a model for the development of cell surface asymmetry.

Three chitin synthase (CS)[1] activities (CSI, II, and III) have been identified in *S. cerevisiae* (Bulawa, 1993; Cabib et al., 1982; Orlean, 1987; Sburlati and Cabib, 1986). All three enzymes are membrane associated and catalyze the synthesis of chitin chains from UDP-*N*-acetylglucosamine. Chs1p is required for CSI activity (Bulawa et al., 1986). CSII activity is encoded by the *CHS2* gene (Silverman et al., 1988). CSIII activity requires the function of *CHS3* (recently renamed from *CAL1/CSD2/DIT101/KTI2*; Cid et al., 1995), which is the presumed catalytic subunit, as well as *CHS4* (*CAL2/CSD4*) and *CHS5* (*CAL3*) (Bulawa, 1992,

Address all correspondence to Randy W. Schekman, Department of Molecular and Cell Biology, Howard Hughes Institute, University of California, Berkeley, Berkeley, CA 04720. Tel.: (510) 642-5686. Fax (510) 642-7846.

1. *Abbreviations used in this paper*: CS, chitin synthase; CWP, cell wall protein; DAPI, 4′,6-diamidino-2-phenylindole; GST, glutathione-*S*-transferase; HA, hemagglutinin; nt, nucleotide; ORF, open reading frame; PGK, phosphoglycerate kinase; PIC, protease inhibitor cocktail: TEA, triethanolamine.

1993; Roncero et al., 1988). Hydropathy analysis of the Chs1p, Chs2p, and Chs3p sequences reveals the presence of multiple putative membrane-spanning domains in each polypeptide (Bulawa, 1992; Bulawa et al., 1986; Silverman, 1989), which is consistent with the idea that chitin synthases polymerize and extrude chitin chains across the plasma membrane from an intracellular source of UDP-*N*-acetylglucosamine.

In vivo, CSI, II, and III are differentially regulated to serve unique requirements for chitin synthesis during various times in the cell cycle. Genetic analyses of *chs1*, *chs2*, and *chs3* mutants and various double mutant combinations suggest that Chs2p synthesizes the chitin disk of the primary division septum at the end of mitosis, whereas Chs3p lays down the chitin ring before bud emergence (Shaw et al., 1991). Chs1p may repair the cell wall in the birth scar, to counteract the effects of excessive chitin hydrolysis by chitinase (Cabib et al., 1989). Whereas not one of the three chitin synthases is absolutely essential for growth, the simultaneous loss of Chs2p and Chs3p is lethal (Shaw et al., 1991).

How are the chitin synthases regulated to achieve the timed, localized deposition of chitin? In vitro, all three chitin synthases have been reported to display zymogenic properties, reflected by an increase in activity after limited proteolysis (Choi et al., 1994*b*; Durán and Cabib, 1978; Sburlati and Cabib, 1986). Based on the zymogenic properties of the chitin synthases, Cabib et al. (1982) proposed a localized activation model. According to this model, the chitin synthase zymogens are uniformly distributed throughout the plasma membrane. Spatially and temporally regulated localization of an activator would restrict chitin synthase activity to distinct regions of the cell surface. However, the physiological activator(s), if any, have not been identified, and there is no evidence for conversion from a zymogenic precursor in vivo.

An alternative model suggests that direct localization of the chitin synthases during specific points in the cell cycle would account for regulated chitin deposition. Correct timing of localization could result from cell cycle–regulated synthesis coupled to rapid degradation. Measurements of CSII activity in synchronized cells as well as in cells harboring an inducible copy of *CHS2* are consistent with this mechanism (Choi et al., 1994*a*). Alternatively, timed localization could be achieved by regulating the machinery required for delivery or retention of the chitin synthase proteins at the region of the mother-bud neck.

One of the most intriguing facets of regulated chitin synthesis is the report of an intracellular membrane fraction termed chitosomes (Flores Martinez and Schwencke, 1988; Leal-Morales et al., 1988). Chitosomes are ~40 to 100 nm in diameter, have a buoyant density of ~1.15 g/ml (34 to 35% sucrose [wt/wt]), and have been reported to contain ~50% of total chitin synthase I activity (Flores Martinez and Schwencke, 1988; Leal-Morales et al., 1988). Because transport of proteins to the cell surface via the secretory pathway occurs rapidly, vesicular intermediates are rapidly consumed and are difficult to detect at steady state, unless a secretory block is imposed (Novick et al., 1980). Thus, it is surprising to find an internal chitin synthase-containing compartment at steady state. It has been proposed that chitosomes are specialized carriers used for the delivery of chitin synthases to specific domains of the cell surface (Bartnicki-Garcia, 1990). However, the physiological role of chitosomes remains unknown, and the biogenesis of the individual chitin synthases and the relationship of chitosomes to the known secretory pathway have not been addressed.

In this paper, we have determined the subcellular localization of Chs2p and Chs3p using indirect immunofluorescence microscopy using either a polyclonal antibody directed against Chs3p or cells expressing a functional, integrated, epitope-tagged *CHS2*. In addition, we have examined the biogenesis of Chs2p and Chs3p through the yeast secretory pathway, as well as the distribution of Chs2p and Chs3p in chitosomes. We present evidence that spatially regulated chitin synthesis is achieved by the specific localization of chitin synthase enzymes. We also demonstrate that the timing of Chs2p and Chs3p localization is accomplished by distinct mechanisms, and we present evidence that Chs2p and Chs3p have different fates after endocytosis.

Materials and Methods

Strains, Growth Conditions, and Reagents

S. cerevisiae strains used in this study are listed in Table I. Yeast cells were grown in synthetic or rich media (Sherman, 1991) at 30°C, or at 24°C for temperature-sensitive strains. Mating, sporulation, and tetrad dissection were performed using standard techniques (Sherman and Hicks, 1991). DNA manipulations in *Escherichia coli* and DNA blot hybridization were performed as described in Ausubel et al. (1987–1995). PCR was carried out using either Taq (Boehringer Mannheim Biochemicals, Indianapolis, IN) or Pfu polymerase (Stratagene, La Jolla, CA) according to the manufacturer's instructions. Yeast transformation was accomplished using standard methods (Ausubel et al., 1987–1995).

chs2::TRP1 (pCHS2W; Bulawa and Osmond, 1990) and *chs3-8::LEU2* (previously *csd2-8::LEU2*; pCS2-D2b; Bulawa, 1992) disruption constructs, and plasmids containing *CHS2* (pSS352ΔXba; Bulawa and Osmond, 1990) and *CHS3* (pCSD2-15; Bulawa, 1992) were gifts from Christine Bulawa (Myco Pharmaceuticals, Inc., Cambridge, MA). The disruption constructs were transformed into YPH499 and YPH500 (Sikorski and Hieter, 1989) to generate JCY302 and JCY305 (both *chs2::TRP1*) and JCY303 and JCY306 (both *chs3-8::LEU2*). The ~4.8-kb XbaI–HindIII insert from pSS352ΔXba was subcloned into pRS316 (Sikorski and Hieter, 1989) and pBSSK(+) (Stratagene) to generate pJC308 and pJC323, respectively. Nucleotide coordinates for the *CHS2* and *CHS3* genes are according to Silverman (1989) and Bulawa (1992).

A plasmid containing *PMA1HA* (Harris et al., 1994) was a gift from James Haber (Department of Biology and Rosenstiel Center, Brandeis University, Waltham, MA). Strains Z106-2C and Z107-11D, containing *PMA1HA* integrated at the *PMA1* locus, are described elsewhere (Ziman et al., 1996). The YPH499 and YPH500 strains and the pRS series of yeast vectors have been described (Christianson et al., 1992; Sikorski and Hieter, 1989). Other strains are described below or were constructed from the described strains and other strains listed in Table I by conventional genetic crosses.

Mouse 9E10 anti-myc mAb (Evan et al., 1985) and 12CA5 anti–hemagglutinin (HA) mAb (Wilson et al., 1984) ascites fluid, and antibodies against Sec13p (Pryer et al., 1993), phosphoglycerate kinase (PGK) (Baum et al., 1978), Sec61p (Stirling et al., 1992), the 33-kD cell wall protein (CWP) (Sanz et al., 1987), and tubulin (gift of the Thorner lab, this department) were used in this work.

Enzymes for the manipulation of DNA were purchased from New England Biolabs (Beverly, MA) or Boehringer Mannheim Biochemicals, unless indicated. Protease inhibitors were purchased from Boehringer Mannheim Biochemicals or Sigma Chemical Co. (St. Louis, MO). ^{35}S-Pro-mix was purchased from Amersham Corp. (Arlington Heights, IL). Other chemicals were purchased from Sigma Chemical Co., unless indicated.

Construction of CHS2MYC

The ~260-bp DraI–EcoRI insert from pJR1265 (pBSKS(+)-6myc; kindly

Table I. Strains Used in This Study

Name	Genotype*		Source‡
YPH499	*MAT***a**	*ura3 trp1 leu2 his3 lys2 ade2*	1
YPH500	*MATα*	*ura3 trp1 leu2 his3 lys2 ade2*	1
DK499	*MAT***a** *bar1*	*ura3 trp1 leu2 his3 lys2 ade2*	2
JCY302	*MAT***a** *chs::TRP1*	*ura3 trp1 leu2 his3 lys2 ade2*	3
JCY305	*MATα chs2::TRP1*	*ura3 trp1 leu2 his3 lys2 ade2*	3
JCY303	*MAT***a** *chs3-8::LEU2*	*ura3 trp1 leu2 his3 lys2 ade2*	3
JCY306	*MATα chs3-8::LEU2*	*ura3 trp1 leu2 his3 lys2 ade2*	3
JCY311	*MAT***a**/*α chs2::TRP1*/+ *chs3-8::LEU2*/+	*ura3 trp1 leu2 his3 lys2 ade2*	3
JCY330	*MAT***a** *CHS2MYC*	*ura3 trp1 leu2 his3 lys2 ade2*	3
JCY366	*MAT***a** *bar1 CHS2MYC*	*ura3 trp1 leu2 his3 lys2 ade2*	3
Z106-2C	*MAT***a** *PMA1HA*	*ura3 trp1 leu2 his3 lys2 ade2*	4
Z107-11D	*MATα PMA1HA*	*ura3 trp1 leu2 his3 lys2 ade2*	4
JCY411	*MAT***a** *chs3Δ::HIS3 PMA1HA*	*ura3 trp1 leu2 his3 lys2 ade2*	3
RSY620	*MAT***a** *pep4::TRP1*	*ura3 trp1 leu2 his3 ade2*	6
JCY380	*MATα CHS2MYC PMA1HA*	*ura3 trp1 leu2 his3 ade2*	3
JCY381	*MATα pep4::TRP1 CHS2MYC PMA1HA*	*ura3 trp1 leu2 his3 ade2*	3
RSY782	*MATα sec1-1*	*ura3 his4*	6
JCY396	*MATα sec1-1 CHS2MYC PMA1HA*	*ura3 trp1 leu2 his3 ade2*	3
JCY397	*MAT***a** *CHS2MYC PMA1HA*	*ura3 trp1 leu2 his3 ade2*	3
JCY398	*MAT***a** *sec1-1 CHS2MYC PMA1HA pep4::TRP1*	*ura3 trp1 leu2 his3 ade2*	3
JCY400	*MAT***a** *CHS2MYC PMA1HA pep4::TRP1*	*ura3 trp1 leu2 his3 ade2*	3
JCY2053	*MAT***a** *bar1 end4-1*	*ura3 leu2 his3*	2
JCY389	*MATα end4-1 CHS2MYC PMA1HA*	*ura3 trp1 leu2 his3 lys2 ade2*	3
JCY390	*MATα CHS2MYC PMA1HA*	*ura3 trp1 leu2 his3 lys2 ade2*	3
DDY593	*MAT***a** *bar1*	*ura3 leu2 his4*	5
DDY594	*MAT***a** *end3-1 bar1*	*ura3 leu2 his4*	5
DDY595	*MAT***a** *end4-1 bar1*	*ura3 leu2 his4*	5

* *chs2::TRP1:CHS2MYC:URA3*, *CHS2MYC*; *pma1::PMA1HA:LEU2*, *PMA1HA*.
‡ Sources: 1: Sikorski and Heiter (1989); 2: Thorner lab, this department; 3: this work; 4: Michael Ziman; 5: Drubin lab, this department; 6: lab strain collection.

provided by Randy Hampton, Department of Biology, University of California, San Diego) was inserted at the BstBI site (near the NH_2 terminus of Chs2p) in pJC323. Before ligation, both DNAs were treated with Klenow polymerase to fill in the 5′ overhangs left by EcoRI and BstBI digestion. The resulting plasmid, pJC324, encodes a protein containing 6 tandem repeats of the myc epitope after Ser-11 of Chs2p. The HindIII–XbaI fragment of pJC324 containing *CHS2MYC* was subcloned into pRS426, pRS316, and pRS306 (Christianson et al., 1992; Sikorski and Hieter, 1989) to generate pJC327, pJC328, and pJC329, respectively. Strains expressing *CHS2MYC* plasmids were tested in immunoblots and in metabolic labeling/immunoprecipitation experiments. Only one specific protein species of the expected size (~120 kD) was detected. This protein was dependent on *CHS2MYC* and was overproduced in strains harboring a high-copy *CHS2MYC* plasmid.

To test for functionality of *CHS2MYC*, we transformed a *chs2::TRP1*/+ *chs3-8::LEU2*/+ double heterozygote (JCY311) with pJC308, pJC328, or the control vector pRS316. The resulting Ura^+ transformants were sporulated and subjected to tetrad analysis. We were unable to recover the *chs2::TRP1 chs3-8::LEU2* double mutant unless the same spore carried either pJC308 or pJC328. These double mutants were dependent on the plasmid because colonies did not form when the strains were streaked on medium containing 5-fluoroorotic acid.

We subsequently constructed a strain in which the only functional copy of *CHS2* is *CHS2MYC*. pJC329 was digested with Bsu36I (which cuts in *CHS2*) and transformed into JCY302 (*chs2::TRP1*). The resulting strain, JCY330 (*chs2::TRP1:CHS2MYC:URA3*, referred to henceforth as *CHS2MYC*), was verified by DNA blot hybridization. JCY330 displayed normal morphology and a growth rate equivalent to wild type, whereas JCY302 cells were clumpy (due to a defect in cell separation) and grew slowly.

Construction of CHS2MYC-mSUC2 Fusions

We used PCR to add HindIII sites to *CHS2MYC* to create two in-frame fusions of Chs2p-myc with mature invertase (encoded by *mSUC2*). Primers 2-1 (5′ GGC CAT TGT CGT TTC AAG G 3′; nucleotide (nt) 3285–3302) and 2-13 (5′ CAA TGC TCT AGA AAG CTT GGC CCT TTT TGT GGA AAA C 3′; underlined sequence represents nt 3706 to 3723 of *CHS2*) were used to amplify a ~0.45-kb fragment from pJC328. The PCR product was cut with Bsu36I (at nt 3339) and XbaI (site in primer 2-13) and subcloned into pJC324, replacing the original Bsu36I–XbaI fragment, to make pJC333. The HindIII insert (containing the modified *CHS2* sequence) from this plasmid was subcloned into the vector pSEYc306 (*CEN4-ARS1 URA3 mSUC2*) (Johnson et al., 1987) to create pJC334 (*CHS2MYC[G963]-mSUC2*). In this construct, QAFTNETSD . . . (QAF from the added HindIII site; underlined residues begin with amino acid 3 of mature invertase) was added to the last amino acid (G963) of Chs2p. Note that the amino acid numbers correspond to Chs2p and not to Chs2p-myc. Primers 2-1 and 2-12 (5′ CAA TGC TCT AGA AAG CTT GAC CAT TGT CAG TAT CTT G 3′; underlined sequence represents nt 3526 to 3543 of *CHS2*) were used in an analogous procedure. The PCR product was cut with Bsu36I and XbaI and subcloned into pJC329, replacing the original Bsu36I–XbaI fragment, to make pJC335. The HindIII insert from pJC335 was subcloned into pSEYc306 to create pJC336 (*CHS2MYC[G903]-mSUC2*). The added amino acids (QAFTNETSD . . .) are identical to the additions in pJC334, except that the fusion junction is after G903 of Chs2p.

Construction of chs3Δ::HIS3, a Complete Deletion of CHS3

We used PCR to synthesize the linear DNA fragment used to construct *chs3Δ::HIS3*, which lacks the entire Chs3p open reading frame (ORF). Primer "upstream" (5′ GGT CCT GTT TAG ACT ATC CGC AGG AAA GAA ATT AGA AAG AGC TTG GTG AGC GCT 3′) was designed to join 36 bp corresponding to the region just upstream of the Chs3p ORF (from nt −36 to −1) with the 5′ end of *HIS3* (from nt 199 to 216 of pRS423, underlined). Primer "downstream" (5′ GTA AGT ATC ACA GTA AAA ATA TTT TCA TAC TGT CTA TCC GTC GAG TTC AAG AGA 3′) was designed to join 36 bp corresponding to the region just downstream of the Chs3p ORF (from nt 4087 to 4122) with the 3′ end of *HIS3* (from nt 1368 to 1351 of pRS423, underlined). These primers were used to amplify a ~1.2-kb fragment from pRS423. This PCR product was transformed into Z106-2C. His^+ transformants were selected and tested for temperature sensitivity, resistance to 0.5 mg/ml Calcofluor, and

anti-Chs3p immunoreactivity. JCY411, which was derived from this procedure, did not grow at 37°C, was resistant to 0.5 mg/ml Calcofluor, and lacked the ~130-kD band found in Z106-2C (*CHS3*) when analyzed by immunoblot with anti-Chs3p antibodies.

Generation and Affinity Purification of Polyclonal Anti-Chs3p Antibodies

We raised antibodies against a glutathione-*S*-transferase (GST)–CHS3N fusion protein containing the first 171 amino acids of Chs3p attached to the COOH terminus of GST. pJC322 was constructed by subcloning a BamHI–EcoRI fragment of Chs3p synthesized by PCR into pGEX2T (Smith and Johnson, 1988). The primers used in the PCR were chs3Bam (5′ CCG GAT CCA TGA CCG GCT TGA ATG G 3′; nt 592 to 608 of *CHS3*, underlined), which created a BamHI site before nt 592 of *CHS3*, and chs3RX (5′ CCC TCT AGA GAA TTC CAT CTG CCA AAA TGA CAA 3′; nt 1087 to 1104 of *CHS3*, underlined), which added an EcoRI site after nt 1104 of *CHS3*.

GST and GST–CHS3N proteins were induced with 0.5 mM isopropyl-thio-β-D-galactoside for 3 h at 30°C and purified from *E. coli* using glutathione-agarose as described (Ausubel et al., 1987–1995). Rabbits were immunized with GST–CHS3N according to Louvard et al. (1982). For affinity purification, 4–5 mg of GST or GST–CHS3N were dialyzed into coupling buffer (0.1 M borate + 0.9% NaCl, pH 8.5) and coupled to 1 ml ReactiGel (6×) carbonydiimidazole-activated agarose (Pierce Chemical Co., Rockford, IL) according to the manufacturer's instructions. Before use, the columns were equilibrated with TBS (150 mM NaCl, 50 mM Tris, pH 7.4). Anti-Chs3p antiserum (5 ml) was diluted in TBS to 15 ml and passed three times over the GST column to select against anti-GST antibodies. The flow-through fraction was then passed three times over the GST–CHS3N column. The column was washed extensively with TBS/500 mM NaCl, and the anti-Chs3p antibodies were eluted with 0.1 M glycine, pH 2.2, into tubes containing 1/20th vol 2 M Tris, pH 8.0. Fractions (1 ml) were collected, and the peak fractions were tested on immunoblots containing TCA-precipitated proteins from JCY411 (*chs3Δ::HIS3*) and Z106-2C (*CHS3*).

Indirect Immunofluorescence Microscopy

Preparation of cells for immunofluorescence was essentially as described by Chiang and Schekman (1991). Mouse 9E10 anti-myc mAb was used at a 1:500 dilution. Rabbit anti–tubulin Ab was used at a 1:1,000 dilution. Affinity-purified rabbit anti–Chs3p Ab was diluted 1:10 and preabsorbed for 2 h at room temperature against 50 OD_{600}/ml fixed, permeabilized spheroplasts prepared from JCY411 (*chs3Δ::HIS3*). FITC-conjugated goat anti–mouse, TRITC-conjugated goat anti–rabbit, and Cy3 (indocarbocyanine)–conjugated goat anti–rabbit secondary Abs (Jackson ImmunoResearch Laboratories, West Grove, PA) were used at 1:250, 1:1,000, and 1:500, respectively.

For peptide competition experiments, we preincubated the diluted anti-myc mAb (or anti-tubulin Ab) with 0.5 or 5 μg/ml (3 or 30 μM) c-*myc* peptide (Feldheim et al., 1992) for 30 min at room temperature. This mixture was then used for immunofluorescence staining.

Electrophoresis and Immunoblotting

Methods for the preparation of extracts for immunoblot analysis closely followed Ausubel et al. (1987–1995). Samples were denatured at 65°C for 10 min before fractionation on SDS-PAGE (Laemmli, 1970). Immunoblotting by enhanced chemiluminescent detection (Amersham Corp.) was performed according to the manufacturer's instructions, after transfer to a 0.45-μm nitrocellulose filter (Schleicher & Schuell, Inc., Keene, NH).

Metabolic Labeling and Immunoprecipitation

^{35}S metabolic labeling of proteins, glass bead lysis, and immunoprecipitation was performed essentially as described by Feldheim et al. (1992), except that labeled cells were chased with 0.1 vol of 50 mM methionine, 10 mM cysteine, 4% yeast extract, and 2% glucose. 1 to 2 OD_{600} U of cells were typically analyzed for each time point. Cells labeled in the presence of 20 μg/ml tunicamycin were preincubated at 30°C for 20 min.

Membrane Extraction

For membrane extraction experiments (Feldheim et al., 1992), we harvested 75 OD_{600} U of early log-phase cells (OD_{600} = 1–4) and lysed them with glass beads in 1 ml B88 (20 mM K-Hepes, 0.25 M sorbitol, 0.15 M KOAc, 1 mM MgOAc, pH 6.8; Baker et al., 1988) per 100 OD_{600} cells. The lysate was diluted to 25 OD_{600} cell equivalents per ml with B88, and then clarified at 500 *g*. One-fifth of the lysate (15 OD_{600} cell equivalents) was then extracted with 0.5 M NaCl, 2 M urea, 0.1 M Na_2CO_3, pH 11, or 1% TX-100 (each from a 4× stock in B88), or B88 alone, and incubated on ice for 30 min before centrifugation at 100,000 *g* for 30 min in a rotor (TLA100.3; Beckman Instruments, Inc., Palo Alto, CA). High speed supernatant and pellet fractions were collected, denatured, and analyzed by immunoblot with anti-myc, anti-Chs3p, and anti-Sec13p Abs. As expected, Chs2p-myc and Chs3p were membrane bound and were not removed by reagents that extract Sec13p, a peripheral membrane protein (data not shown).

Membrane Fractionation

For analysis of chitosomes, we lysed cells (scales indicated below) according to Makarow (1985), with minor modifications (Nakamoto et al., 1991). Cells grown in yeast extract/peptone/dextrose (YPD) (to OD_{600} = 1–4) were harvested and converted to spheroplasts in HB (1.4 M sorbitol, 50 mM KP_i, pH 7.5, 10 mM NaN_3, 10 mM NaF, 40 mM β-mercaptoethanol), using 200 μg/ml Zymolyase 100T (ICN Biomedicals Inc., Irvine, CA) at 30°C for 30 min. Spheroplasts were resuspended at ~50 OD_{600} cell equivalents per ml and treated with ~1.5 μg Con A/OD_{600} U of cell equivalents in HB + 10 mM $MgCl_2$ at 4°C for 15 min and washed in the same buffer. Con A–coated spheroplasts were lysed by resuspension in triethanolamine (TEA) lysis buffer (0.5 M sorbitol, 25 mM TEA, pH 8.0, 1 mM EDTA) containing a protease inhibitor cocktail (PIC) (1 mM PMSF, 1 μg/ml pepstatin A, 1 μg/ml leupeptin, 0.1 μg/ml chymostatin, 1 μg/ml aprotinin, and 1 mM benzamidine), followed by incubation at 30°C for 10 min.

For differential centrifugation experiments involving radiolabeled cells, we radiolabeled and harvested 2.5 to 5 OD_{600} U of cells for each point. After conversion into Con A–coated spheroplasts and TEA lysis, the extract was centrifuged at 500 *g* for 5 min and at 10,000 *g* for 10 min in a refrigerated microcentrifuge. The supernatant was not removed between these steps. The S10 was transferred to a separate tube, and the pellet was resuspended in an equal volume of TEA lysis buffer + PIC. Denaturing immunoprecipitation buffer was added to 1× (1% SDS, 50 mM Tris, pH 7.5, 1 mM EDTA, 1 mM PMSF), and the samples were heated at 65°C for 10 min and immunoprecipitated as described above.

For sucrose equilibrium density gradient centrifugation, we harvested 250 OD_{600} U of cells, converted them to Con A–coated spheroplasts, and lysed them in TEA as described above. This extract was clarified at 500 *g*, and subsequently centrifuged at 20,000 *g* in a rotor (HB-4; DuPont/Sorvall, Wilmington, DE). An aliquot (500 μl) of the resulting S20 was layered onto a 30 to 55% (wt/wt) sucrose/TEA gradient, followed by centrifugation in a rotor (SW41; Beckman Instruments, Inc.) at 150,000 *g* for 24 h. The gradient was prepared by successively layering 0.5 ml 55%, 2.0 ml 50%, 2.5 ml 45%, 2.5 ml 40%, 2.5 ml 35%, and 1.75 ml 30% (wt/wt) sucrose (in 10 mM TEA-acetate, pH 7.2, 1 mM EDTA + PIC) in a 12.5-ml tube (344059; Beckman Instruments, Inc.). Fractions (0.4 ml) were collected from the top at 0.5 ml/min using a gradient fractionator (model 640; ISCO, Lincoln, NE).

Results

Chs2p-myc and Chs3p Enter the Secretory Pathway through the ER

To examine the role of the secretory pathway in the biosynthesis of the chitin synthases, we raised polyclonal antibodies against Chs3p and constructed a functional, integrated, myc_6-tagged *CHS2* (see Materials and Methods). Chs2p-myc and Chs3p behaved as integral membrane proteins in membrane extraction experiments (data not shown; see Materials and Methods). One marker for entry of membrane proteins into the ER is N-linked glycosylation of Asn residues on luminally exposed Asn-X-Ser/Thr consensus sites. N-linked glycosylation, which is inhibited in vivo by treatment with tunicamycin, reduces the electro-

phoretic mobility of proteins on SDS-PAGE. We metabolically labeled cells with ^{35}S-Pro-mix in the presence or absence of tunicamycin, followed by immunoprecipitation with anti-myc or anti-Chs3p Abs. Chs3p precipitated from tunicamycin-treated cells migrated faster than Chs3p from control cells (Fig. 1 *A*, *right*), indicating that it undergoes N-linked glycosylation in the ER. We also found evidence for Chs3p glycosylation in Con A–Sepharose binding experiments (data not shown).

We were unable to detect a similar mobility shift with Chs2p-myc (Fig. 1 *A*, *left*, lanes *1* and *2*). Its glycosylation consensus sites are upstream of the first putative transmembrane domain and probably face the cytoplasm. Alternatively, limited glycosylation of this large protein might result only in a slight, undetectable shift in mobility. To facilitate our analysis, we constructed two COOH-terminal fusions of Chs2p-myc to a version of the secretory protein invertase lacking its native signal sequence (mature invertase, encoded by *mSUC2*). Invertase contains 12 to 13 glycosylation sites (Trimble and Maley, 1977), but in the absence of a signal sequence, it cannot enter the ER for glycosylation. When mature invertase was fused to the COOH terminus of Chs2p-myc (*CHS2MYC[G963]-mSUC2*, expressed from a *CEN* plasmid), the migration of the hybrid protein on SDS-PAGE was unaffected by tunicamycin (Fig. 1 *A*, *left*, lanes *3* and *4*). However, when invertase was inserted upstream of the last predicted transmembrane domain of Chs2p-myc (resulting in a deletion of this last domain: *CHS2MYC[G903]-mSUC2*, expressed from a *CEN* plasmid), the hybrid protein displayed a tunicamycin-dependent mobility shift (Fig. 1 *A*, *left*, lanes *5* and *6*). Thus, Chs2p-myc can direct translocation of a heterologous protein into the ER, suggesting that Chs2p normally enters the ER during its biogenesis. In addition, the differential glycosylation of the two fusions suggests that the COOH terminus of Chs2p faces the cytosol, whereas the loop upstream of the last transmembrane domain faces the lumen of the ER.

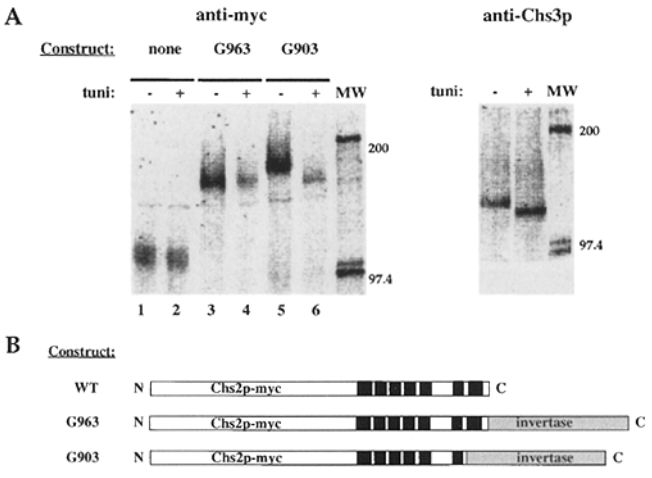

Figure 1. Evidence that Chs2p-myc and Chs3p enter the ER. (*A*, *left*) YPH499 strains expressing *CHS2MYC(G963)-mSUC2* (pJC334) (lanes *3* and *4*), *CHS2MYC(G903)-mSUC2* (pJC336) (lanes *5* and *6*), or the integrated *CHS2MYC* (JCY330) (lanes *1* and *2*) were incubated for 15 min and labeled for 20 min in the presence (lanes *2*, *4*, and *6*) or absence (lanes *1*, *3*, and *5*) of 20 μg/ml tunicamycin (*tuni*) at 30°C. (*A*, *right*) JCY380 was labeled by the same procedure. Proteins were immunoprecipitated using either the anti-myc mAb (*A*, *left*) or anti-Chs3p serum (*A*, *right*). The positions of the molecular weight markers (in kD) are shown. (*B*) Diagrammatic representation of Chs2p-myc–invertase fusion proteins. (*Black boxes*) Possible membrane-spanning domains.

Chs2p-myc and Chs3p Localize to the Mother-Bud Neck at Specific But Distinct Times during the Cell Cycle

To assess the subcellular localization of Chs2p-myc and Chs3p, we performed indirect immunofluorescence using the anti-myc mAb 9E10 and affinity-purified anti-Chs3p antiserum, respectively. The anti-Chs3p Abs were first preadsorbed against fixed, permeabilized *chs3Δ::HIS3* cells. Both antibodies recognized a single protein of the predicted molecular mass on immunoblots of whole cell extracts (data not shown; see Materials and Methods).

Indirect immunofluorescence microscopy of *CHS2MYC* cells revealed heterogeneous staining. Some cells displayed perinuclear staining, a hallmark pattern of ER localization (Fig. 2 *C*). We also detected internal punctate staining in some unbudded cells (Fig. 2 *B*). Most notably, in a minor population of cells, Chs2p-myc was restricted to the neck region between the mother and the bud (Fig. 2, *A*, *D*, and *E*). These three patterns of staining were specific because they were not observed when the anti-myc mAb was omitted (data not shown) or when a strain lacking the myc epitope was stained (Fig. 2 *F*). Furthermore, inclusion of a c-*myc* peptide (Feldheim et al., 1992) abolished Chs2p-myc but not tubulin staining (data not shown).

The heterogeneity of staining suggested that Chs2p-myc neck localization might be cell cycle regulated. Analysis of 4′,6-diamidino-2-phenylindole (DAPI)–stained nuclei supported this idea because Chs2p-myc neck staining was seen predominantly in large-budded cells late in nuclear division. In addition, double-labeling experiments with anti-tubulin Abs confirmed that the localization of Chs2p-myc to the mother-bud neck occurred only during anaphase and telophase. All cells with neck staining had fully extended or disassembling spindles (see Figs. 2 and 4). The timing of Chs2p-myc localization to the mother-bud neck is consistent with its known role in septum formation after mitosis.

Cells decorated with the anti-Chs3p antibody also displayed several patterns. Most cells had internal punctate staining. In some cells, we found Chs3p localized in a ring on the cell surface (Fig. 3, *arrows*). As with Chs2p, the heterogeneity appeared to be due to cell cycle–regulated localization. The rings were found in small-budded cells and outlined the neck between the mother and the bud. Similar rings were observed in unbudded cells. In most cells, this ring resembled a crescent at the edge of the cell, and we were only able to distinguish the ring pattern in cells that had settled on the slide with the ring parallel to the plane of focus. In a minor population of large-budded cells, Chs3p staining resembled that of Chs2p-myc (Fig. 3, *arrowhead*), as Chs3p was localized in the neck region between the mother and the large bud. Quantification revealed that 92.5% of cells with neck-localized Chs3p were unbudded or small-budded cells (Fig. 4); the remaining

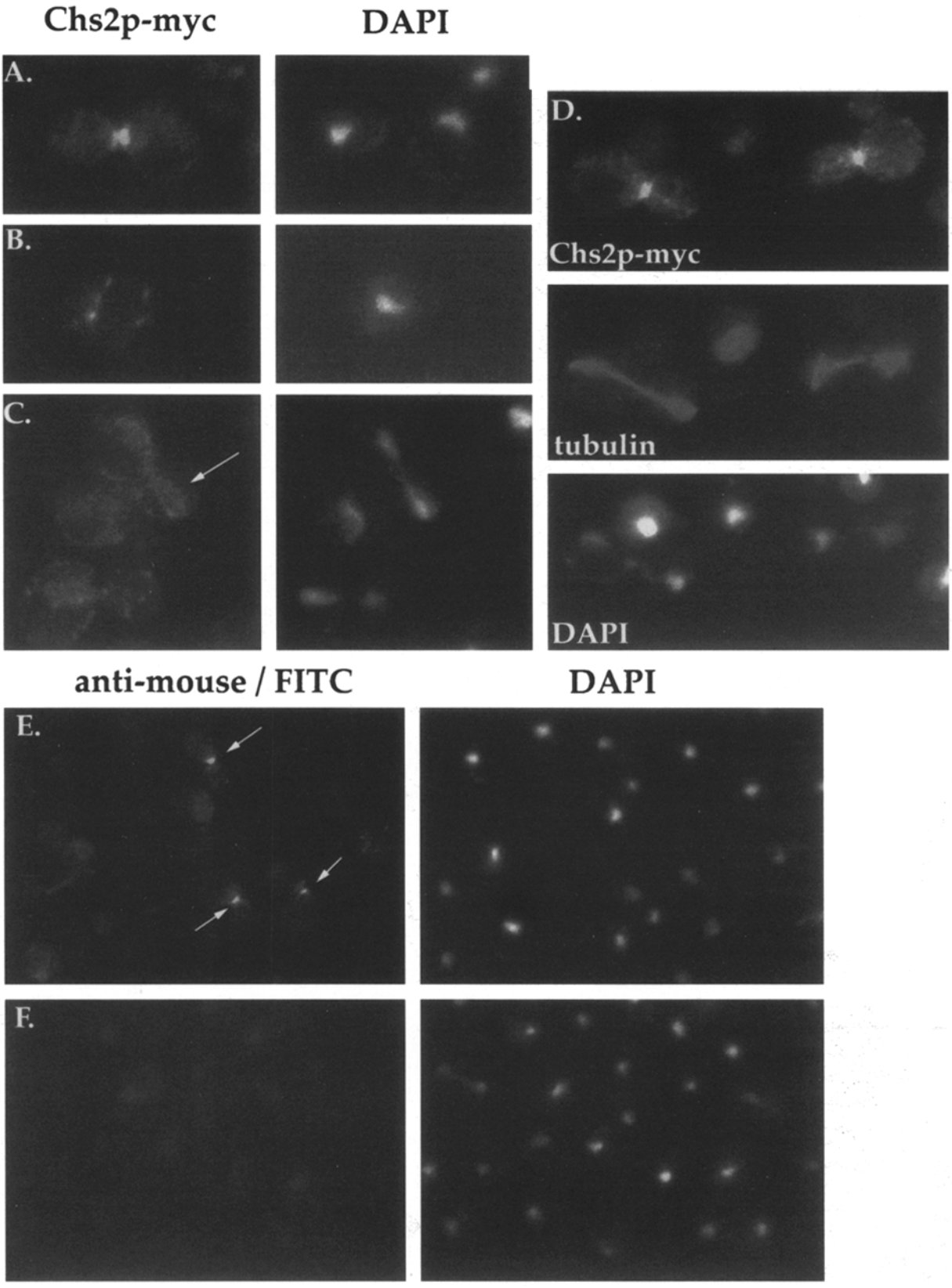

Figure 2. Localization of Chs2p-myc in wild-type cells. *CHS2MYC* cells (JCY330) (*A–E*) or cells lacking *CHS2MYC* (strain YPH499) (*F*) were labeled with anti-myc mAbs in combination with a FITC-conjugated secondary Ab. (*A*) Dividing cell with Chs2p-myc at the mother-bud neck. (*B*) Unbudded cell with punctate staining. (*C*) Large-budded cell with perinuclear staining (*arrow*). Double labeling (*D*) was done with anti-tubulin Abs in combination with a Cy3-conjugated secondary Ab. The only cells that have Chs2p-myc at the mother-bud neck are in anaphase or telophase. Cells with Chs2p-myc at the mother-bud neck (*E*, *arrows*). Neck staining is not seen when cells lacking *CHS2MYC* (strain YPH499) are stained (*F*).

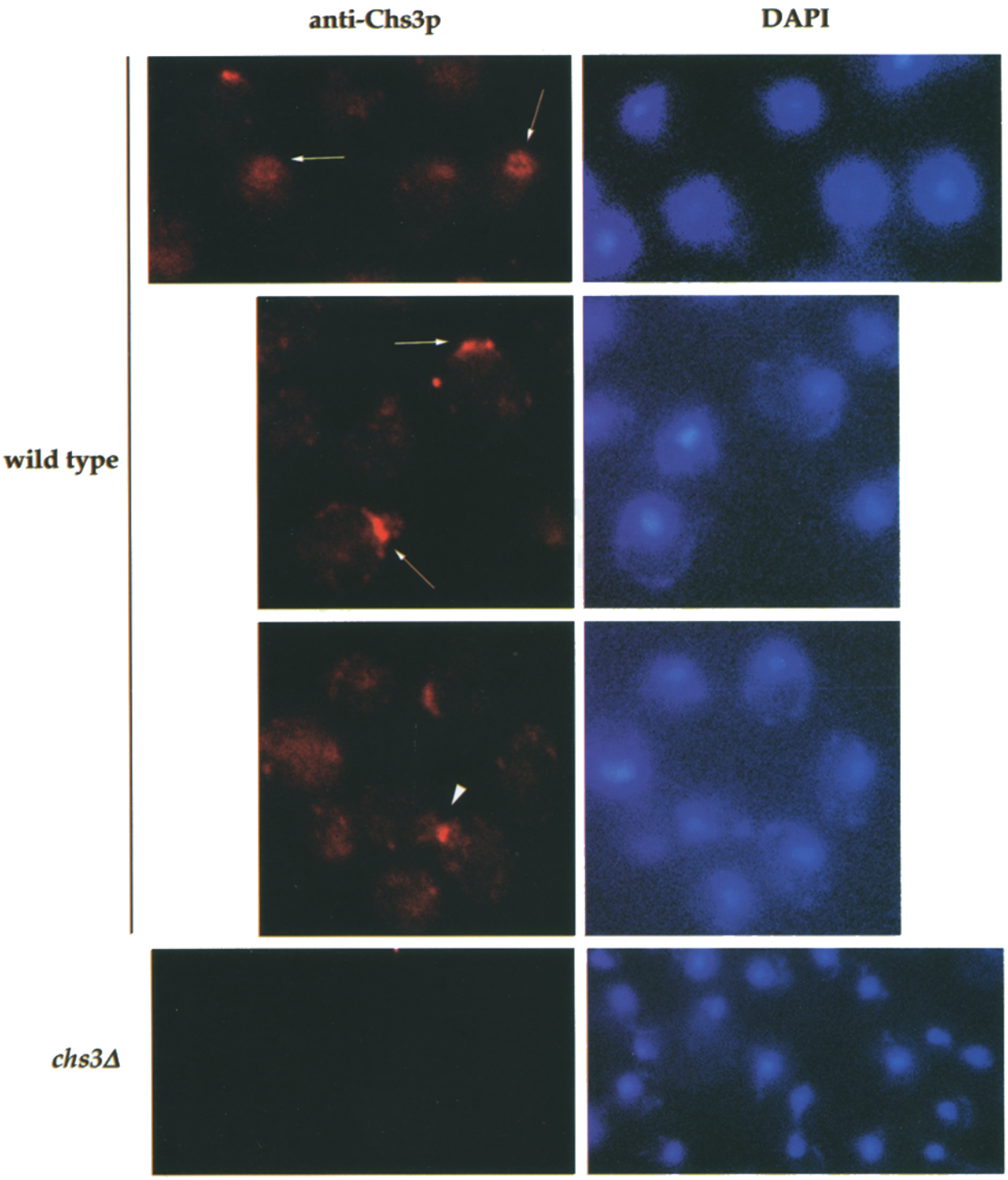

Figure 3. Localization of Chs3p in wild-type cells. Z106-2C cells were labeled with affinity-purified anti-Chs3p antiserum followed by a Cy3-conjugated secondary Ab (see Materials and Methods). (*Arrows*) Chs3p localizes to a ring on the surface of unbudded and small budded cells. (*Arrowhead*) Chs3p is occasionally found at the mother-bud neck in mitotic cells. (*Bottom*) *chs3Δ::HIS3* cells (JCY411) were also labeled as a specificity control.

cells had large buds. We rarely, if ever, found any medium-budded cells with Chs3p localized to the neck region.

Several controls attest to the specificity of the Chs3p localization. When anti-Chs3p antibodies were omitted from the procedure, there was only light, diffuse cytoplasmic staining (data not shown). In addition, affinity-purified, preadsorbed antiserum from a different rabbit resulted in similar staining patterns (data not shown). Finally, *chs3Δ::HIS3* cells (Fig. 3, *bottom*; and data not shown) did not exhibit the patterns observed in wild-type cells. In some cells, we found large spots associated with the nucleus, as judged by colocalization with DAPI staining material. A

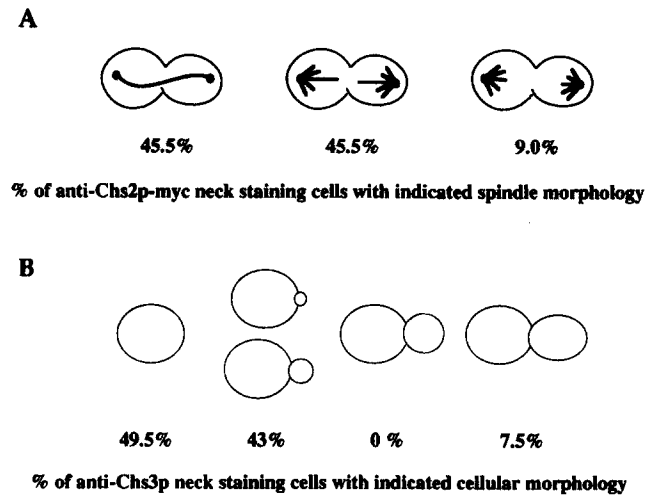

Figure 4. Cell cycle stages of cells with Chs2p-myc or Chs3p neck localization. For Chs2p-myc, cells were double labeled with anti-tubulin Abs. In each case, the slides containing stained samples were scanned for cells localizing Chs2p-myc (*A*, $n = 77$) or Chs3p (*B*, $n = 105$) to the neck. These cells were then scored for cell cycle stage by bud size (*B*) or by spindle morphology (*A*). Numbers indicate the percentage of cells with neck staining at a particular stage.

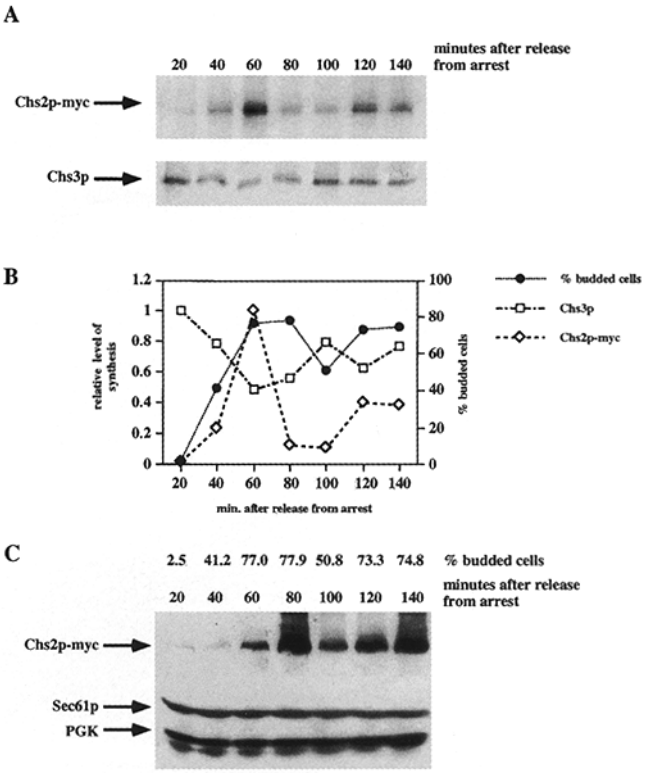

Figure 5. Analysis of Chs2p-myc and Chs3p synthesis in synchronized cells. JCY366 (*MAT***a** *bar1 CHS2MYC*) cells were arrested with 80 ng/ml α-factor for 3 h at 30°C. The cells were washed into fresh medium (lacking α-factor) and held on ice. Aliquots were removed every 20 min and shifted to 30°C. After a total of 120 min, cells were washed into sulfate-free medium and incubated for an additional 20 min. One half of the cells was then harvested for immunoblot analysis with antisera against myc, Sec61p, and PGK (a small portion was also scored for the percentage of budded cells) (*C*). The remaining half was radiolabeled with ^{35}S-Pro-mix for 20 min, lysed, and immunoprecipitated with anti-myc (*A*, *upper*) or anti-Chs3p Abs (*A*, *lower*). (*B*) Quantification of *A*. The times in *A* and *B* indicate the time (in min) after release from arrest when the labeling was initiated. Band intensities (in phosphorimage units) were standardized for the amount of input radioactivity. The time point with the highest intensity for each protein was arbitrarily assigned a value of 1, and other points were calculated relative to the peak.

light cytoplasmic punctate pattern, which was much less pronouced that the punctate staining observed in wild-type cells, was also seen in control *chs3Δ::HIS3* cells.

Regulated Synthesis May Account for the Timing of Chs2 Localization, but Not for That of Chs3p

A striking feature of the Chs2p-myc and Chs3p staining patterns was the apparent restriction of neck localization to specific times during the cell cycle. These proteins might be present only at those times, due to regulated synthesis and/or degradation, or other factors responsible for their localization might be cell cycle regulated.

To explore this problem, we analyzed the synthesis and steady state levels of both proteins in synchronized cell populations. *MAT***a** *bar1 CHS2MYC* cells were arrested in late G1 with the mating pheromone α-factor, and then washed into medium lacking α-factor to release the cells from arrest. These cells progressed through the cell cycle in a relatively synchronous fashion, as judged by budded cell counts (Fig. 5 *B*). Samples were taken every 20 min, and each sample was split for immunoblot analysis and for metabolic labeling for 20 min with ^{35}S-Pro-mix followed by immunoprecipitation with anti-myc or anti-Chs3p Abs. The immunoblot analysis clearly showed that Chs2p-myc levels were modulated during the cell cycle. Chs2p-myc levels were barely detectable in early time points (20 and 40 min; Fig. 5 *C*). The levels of Chs2p increased at ~60 min, peaking at 80 min after release (Fig. 5 *C*). At this time, many cells had large buds and were undergoing mitosis, as judged by tubulin staining (data not shown). Subsequently, Chs2p-myc levels dropped after the cells finished dividing.

Analysis of the metabolically labeled cells showed that the synthesis of Chs2p paralleled the steady state protein levels (Fig. 5, *A* and *B*). In contrast, Chs3p was synthesized constitutively (Fig. 5, *A* and *B*), and its steady state levels remained fairly constant over the cell cycle (data not shown; Ziman et al., 1996). Thus, the temporal restriction of Chs3p localization to the bud site and mother-bud neck cannot be explained by the simple regulated synthesis mechanism invoked for Chs2p-myc.

Chs2p-myc Is Rapidly Degraded in a PEP4-dependent Manner, but Chs3p is Metabolically Stable

The rapid fluctuations in Chs2p-myc levels during the cell cycle led us to examine the stability of Chs2p-myc in pulse-chase experiments. Cells expressing Chs2p-myc were metabolically labeled with ^{35}S-Pro-mix, chased, and collected at various times. Cells from each time point were lysed with glass beads and subjected to immunoprecipitation using anti-myc antibody, followed by SDS-PAGE and phos-

phorimagery. Fig. 6 *A* (*top panel*) shows that Chs2p-myc is an unstable protein, decaying with a half-life of ~25 min at 30°C. Furthermore, the degradation of Chs2p-myc did not occur in strains lacking the major vacuolar protease *PEP4* (Hemmings et al., 1981), indicating that Chs2p-myc was delivered to the vacuole soon after its synthesis (Fig. 6 *A*, *top panel*).

We also assessed the stability of Chs3p in *PEP* cells. In contrast to the rapid degradation of Chs2p-myc, Chs3p was metabolically stable, with a half-life significantly >120 min (Fig. 6 *B*).

Chs2p-myc Degradation Is Blocked by Mutations in SEC1 and END4

We took advantage of the rapid degradation of Chs2p-myc to examine the requirements for its delivery to the vacuole. A temperature-sensitive mutation in *SEC1* (*sec1-1*), a gene involved in the delivery of Golgi-derived transport vesicles to the cell surface (Novick et al., 1980), prevented the degradation of Chs2p-myc when the cells were labeled and chased at 37°C (Fig. 6 *A*, *middle panel*). In addition, a mutation in *END4* (*end4-1*), which is required for the internalization step of endocytosis (Raths et al., 1993), also blocked the degradation of Chs2p-myc when cells were incubated at 30° or 37°C (Fig. 6 *A*, *bottom panel*). As previously reported, *sec1-1* and *end4-1* did not block the vacuolar processing of carboxypeptidase Y, which bypasses the cell surface as a result of sorting in the Golgi into vesicles directly targeted for the vacuole (Raths et al., 1993; Stevens et al., 1982; data not shown).

A Fraction of Chs3p Resides in an Internal Compartment Reminiscent of Chitosomes

One of the main issues regarding the biogenesis of the chitin synthases is the role of chitosomes, which have been hypothesized to play a role in the delivery of chitin synthase to a specific area of the cell surface, perhaps in a cell cycle–regulated manner (Bartnicki-Garcia, 1990). We examined chitosomes for the presence of Chs2p-myc and Chs3p.

We analyzed the distribution of Chs2p-myc and Chs3p using the lysis procedure of Makarow (1985) with minor modifications (Nakamoto et al., 1991). Spheroplasts were coated with the tetrameric Con A, which cross-links the plasma membrane, allowing quantitative sedimentation of plasma membrane by differential centrifugation after osmotic lysis in a TEA-based buffer. We applied this method to metabolically labeled cells to investigate if Chs2p-myc and Chs3p reside in an internal compartment. Wild-type cells expressing an HA-tagged plasma membrane ATPase (Pma1p-HA) were labeled with ^{35}S-Pro-mix for 20 min at 30°C and chased for various times. Each sample was converted into Con A–coated spheroplasts, osmotically lysed, and centrifuged at 10,000 *g*. The resulting pellet and supernatant fractions were then counted in a scintillation counter (quantifying the release of radioactivity into the supernatant as a measure of lysis), immunoprecipitated with anti-Chs3p or anti-HA Abs, and analyzed by SDS-PAGE and phosphorimagery. Approximately 30–50% of Chs3p was found in the supernatant fraction (Fig. 7). This slowly sedimenting fraction was relatively devoid of plasma membrane, as judged by the distribution of Pma1p-HA. In similar experiments, we did not find Chs2p-myc in the supernatant (data not shown), a result that is consistent with its rapid endocytosis and degradation in the vacuole.

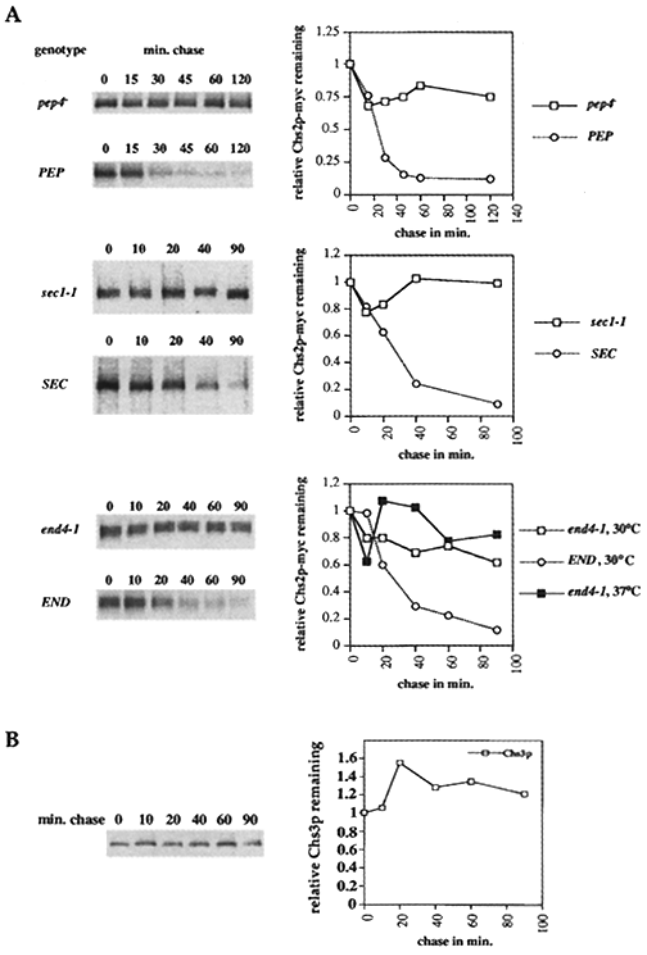

Figure 6. Chs2p-myc, in contrast with Chs3p, is rapidly degraded in a *PEP4*-, *SEC1*-, and *END4*-dependent manner. Cells were labeled for 10 min with ^{35}S-Pro-mix, chased for the indicated times, lysed, and immunoprecipitated for Chs2p-myc (*A*) or Chs3p (*B*). (*A*, *top panel*) Strains JCY380 (*PEP CHS2MYC*) and JCY381 (*pep4*$^-$ *CHS2MYC*) were grown and kept at 30°C throughout the course of the experiment. (*A*, *middle panel*) Strains JCY396 (*sec1-1 CHS2MYC*) and JCY397 (*SEC CHS2MYC*) were grown at 25°C, and then preincubated for 45 min, labeled, and chased at 37°C. (*A*, *bottom panel*) Strains JCY389 (*end4-1 CHS2MYC*) and JCY390 (*END CHS2MYC*) were grown at 25°C, and then preincubated for 45 min, labeled, and chased at 30°C. Quantification of Chs2p-myc stability in *end4-1* at 37°C is also shown in the graph (*A*, *bottom right*). (*B*) JCY380 was grown, labeled, chased at 30°C, and then immunoprecipitated with anti-Chs3p Abs.

From these observations, it appears that Chs3p resides in a small intracellular compartment reminiscent of the previously described chitosomes. Chitosomes did not appear to correspond to ER, Golgi, vacuole, or mitochondria, as judged by immunoblot analysis of sucrose equilibrium density gradients (Ziman et al., 1996). Surprisingly, the distribution of newly synthesized Chs3p in chitosomes did not dramatically change during an extended chase period (Fig. 7). This may reflect a balance in the flow of

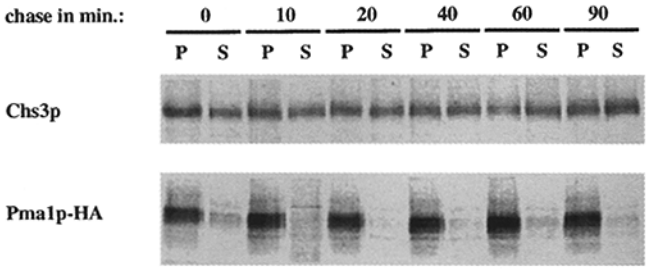

% in supernatant:

Chs3p:	36.8	41.5	48.2	47.8	58.0	56.6
Pma1p-HA:	16.8	14.9	5.7	7.4	13.9	10.0
cpm:	67.8	71.7	75.5	81.8	83.8	82.0

Figure 7. Chs3p is found in an internal compartment called the chitosome. Analysis of the subcellular distribution of newly synthesized Chs3p vs Pma1p-HA. Cells (strain JCY380, grown at 30°C) were labeled for 20 min, chased for the indicated times, converted into Con A–coated spheroplasts, and osmotically lysed in a TEA-based buffer (see Materials and Methods). The lysates (T) were centrifuged at 500 *g* (for 5 min), and subsequently at 10,000 *g* (for 5 min) without transferring the supernatant between centrifugations. The supernatant (*S*) and pellet (*P*) fractions were denatured and subjected to immunoprecipitation using anti-Chs3p and anti-HA Abs. The extent of lysis is indicated by the percentage of total radioactivity (*cpm*) released into the supernatant.

Chs3p into and out of the chitosome membrane (see Discussion).

Chs3p-containing Chitosomes Are Endocytically Derived

Chs3p-containing chitosomes may be derived from the Golgi complex as carriers for the delivery of Chs3p to the cell surface. Alternatively, chitosomes may be endocytically derived. We compared the density of chitosomes with the density of Golgi-derived constitutive secretory vesicles accumulated in *sec1-1* cells by fractionating small membranes through sucrose equilibrium density gradients. Supernatant fractions (20,000 *g*) were prepared from temperature-shifted, Con A–coated *sec1-1* and wild-type spheroplasts and centrifuged to equilibrium in sucrose gradients. As markers for *sec1-1* vesicles, we analyzed Pma1p-HA as well as the secreted 33-kD CWP (Sanz et al., 1987). Pma1p has been shown to accumulate in *sec1-1* vesicles (Holcomb et al., 1988). We measured the distribution of Chs3p, the ER marker Sec61p (Stirling et al., 1992), and the cytosolic marker, PGK (Baum et al., 1978), across both gradients.

In wild-type cells, Chs3p-containing chitosomes equilibrated at ~37–38% (wt/wt) sucrose (Fig. 8 *A*, fraction *12*). Pma1p-HA was not found (Fig. 8 *A*) because the Con A–coating procedure depleted the plasma membrane from the S20 (Fig. 7; data not shown). CWP was soluble and stayed at the top of the gradient (Fig. 8 *A*). In the *sec1-1* gradient, both Pma1p-HA and CWP accumulated in an intracellular pool of constitutive secretory vesicles. These

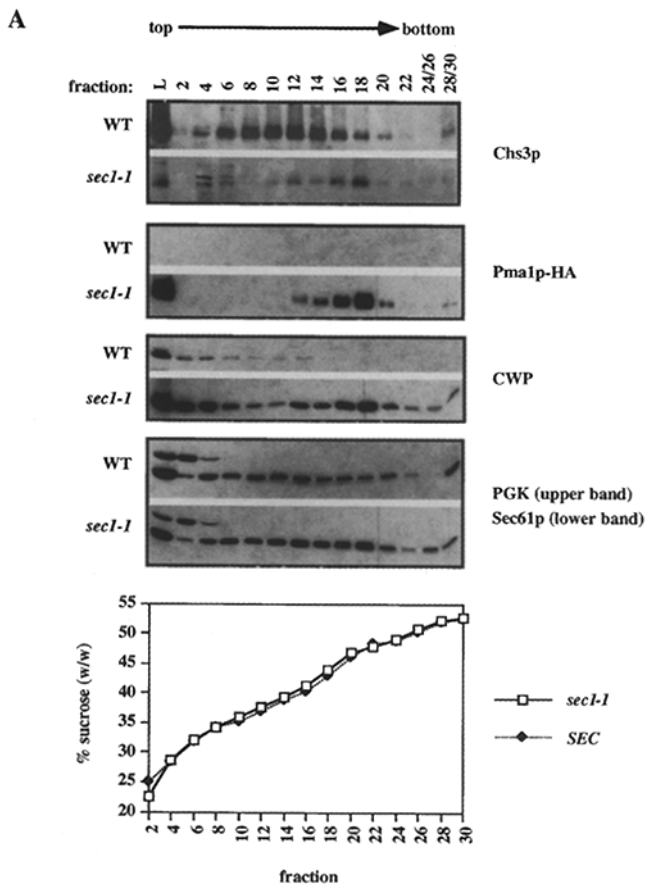

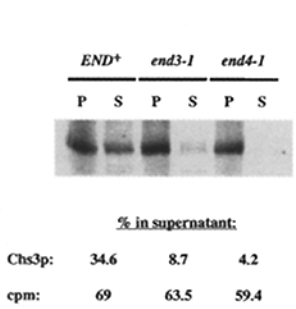

% in supernatant:

Chs3p:	34.6	8.7	4.2
cpm:	69	63.5	59.4

Figure 8. Evidence that chitosomes containing Chs3p are endocytically derived. (*A*) Sucrose equilibrium density gradient fractionation of membranes from JCY400 (*SEC pep4::TRP1*) and JCY398 (*sec1-1 pep4::TRP1*) cells. An S20 (*L*) was loaded onto the top of a 12.5-ml 30 to 55% sucrose/TEA gradient and centrifuged at 150,000 *g* for 24 h (see Materials and Methods). Fractions were collected from the top, TCA precipitated, and analyzed by immunoblotting with antisera against Chs3p, Pma1p-HA, CWP, Sec61p, and PGK. Pma1p-HA is absent from the S20 of *SEC* cells (see Fig. 7). Sucrose concentrations (determined by refractometry) are indicated. (*B*) Differential centrifugation analysis of Chs3p in DDY593 (*END*), DDY594 (*end3-1*), and DDY595 (*end4-1*) cells. Cells were incubated at 37°C for 45 min, radiolabeled with ^{35}S-Pro-mix for 20 min at 37°C, and chased for 60 min at 37°C. Fractionation was performed as described in Fig. 7.

sec1-1 vesicles equilibrated at ~43–44% (wt/wt) sucrose (Fig. 8 *A*, fraction *18*). Notably, the major peak containing Chs3p in *sec1-1* extracts corresponded to the density of the accumulated secretory vesicles (Fig. 8 *A*). The density dif-

ference between the *sec1-1* secretory vesicles and the Chs3p-containing chitosomes from wild-type cells suggests that chitosomes are distinct from constitutive secretory vesicles. In addition, the density shift of Chs3p in wild-type vs *sec1-1* cells indicates that Chs3p is transported to the plasma membrane via vesicles that depend on *SEC1* function.

To determine if chitosomes are endocytically derived, we performed the pulse-chase differential centrifugation analysis of chitosomes in mutants defective in internalization (Raths et al., 1993). Wild-type, *end3-1*, and *end4-1* cells were shifted to 37°C for 45 min, and the cells were radiolabeled with ^{35}S-Pro-mix for 20 min followed by a 60-min chase. This chase time was sufficient to detect the presence of chitosomes (Fig. 7). Cells were then converted into Con A–coated spheroplasts, osmotically lysed, and subjected to a 10,000 *g* centrifugation followed by immunoprecipitation with anti-Chs3p Abs. As expected, chitosomes were readily detected in wild-type cells (Fig. 8 *B*). However, in the *end3-1* and *end4-1* strains, the amount of Chs3p found in chitosomes was diminished (Fig. 8 *B*). Analogous experiments with shorter preshifts (0 or 15 min) of the *end4-1* mutant also showed a reduction in the amount of Chs3p present in the supernatant, although the defect was slightly less severe (data not shown). Since *end3-1* and *end4-1* have been shown to be defective in the internalization step of endocytosis (Raths et al., 1993), we suggest that Chs3p-containing chitosomes are endocytically derived.

Discussion

Timed Localization of the Integral Membrane Proteins Chs2p and Chs3p to the Incipient Bud Site and the Mother-Bud Neck

In this work, we have addressed the mechanism of the spatially and temporally regulated deposition of chitin. Accordingly, we analyzed the biogenesis and determined the subcellular localization of Chs2p and Chs3p, the likely catalytic subunits of chitin synthase II and III, respectively. The most noteworthy feature of the distribution of Chs2p-myc and Chs3p is their localization at the incipient bud site (Chs3p) and at the neck between the mother and the bud. Furthermore, this localization only occurs at distinct points in the budding cycle, and the timing of localization is different between Chs2p-myc and Chs3p. Specifically, Chs2p-myc is found in the mother-bud neck only at the end of mitosis (Figs. 2 and 4). From anti-tubulin double-labeling experiments as well as by DAPI staining of nuclei, we have determined that the localization is restricted to large-budded cells that have completed chromosome separation, which places this event at anaphase/telophase. Chs2p-myc localization to the neck at this time in the cell cycle is consistent with its predicted role in septum formation (Shaw et al., 1991; Bulawa, 1993).

Chs3p appears to be localized to the bud site at different times in the cell cycle (Figs. 3 and 4). Before bud emergence, Chs3p is found in a ring on the cell surface at what probably marks the future site of bud formation. In small-budded cells, this ring remains in the neck at the base of the bud. However, this pattern is transient, as we have not been able to identify cells with medium-sized buds that exhibit this ring. Later, as cells prepare to divide, the reappearance of Chs3p at the mother-bud neck is sometimes detected. After cell separation, the mitotic Chs3p neck staining seems to disappear as the cells enter the next cycle. Localization of Chs3p to the incipient bud site correlates with its proposed role in chitin ring formation (Shaw et al., 1991; Bulawa, 1993). The occasional mitotic neck staining may indicate that Chs3p plays a minor role during septum formation.

S. cerevisiae buds do not emerge at identical sites during successive division cycles. Haploid cells generally bud in an axial pattern, choosing a site immediately adjacent to the location of the previous bud, whereas diploids bud in a bipolar pattern (Chant and Pringle, 1995). If Chs3p rings persisted into a subsequent division cycle, two rings on the surface of small-budded cells, one demarcating the previous bud site and the other positioned at the new site of bud emergence, should be observed. The detection of just a single ring at the base of the new bud implies that the old ring disassembles and then reassembles at the new bud site. We have also observed the same localization pattern in a diploid strain (data not shown). The immunofluorescence localization data, on its own, do not distinguish whether disassembly involves diffusion of Chs3p throughout the cell surface, endocytosis of Chs3p, or both events.

The temporal regulation of Chs2p-myc localization is better understood. Despite the intriguing presence of four consensus Cdc28p phosphorylation sites in the NH_2-terminal 108 amino acids of Chs2p, the main mechanism of control seems to be at the level of cell cycle–regulated synthesis coupled to rapid degradation. This was predicted by Choi et al. (1994*a*) from their measurements of chitin synthase II enzyme activity during the cell cycle or after repressing *CHS2* transcription from the *GAL1* promoter. We have extended their findings by demonstrating that Chs2p-myc protein levels are modulated across the cell cycle, peaking during mitosis and declining shortly afterwards (Fig. 5 *C*). We have also shown in pulse-chase experiments that Chs2p-myc is rapidly degraded, with a half-life of ~25 min at 30°C (Fig. 6 *A*). Finally, we found in pulse-labeling experiments with synchronized cells that synthesis of Chs2p-myc is cell cycle regulated (Fig. 5, *A* and *B*). These findings are consistent with the analysis of *CHS2* mRNA levels during the cell cycle (Pammer et al., 1992). Cell-cycle regulated synthesis of Chs2p coordinated with its rapid degradation thus appears to play an important role in the temporal restriction of Chs2p neck localization to the end of mitosis. The immediate decay of chitin synthase II activity after repression of *GAL1-CHS2* (Choi et al., 1994*a*) strongly suggests that Chs2p degradation can occur at any time in the cell cycle. By determining if localization to the neck can occur when Chs2p is misexpressed at other times in the cell cycle, it may be possible to probe the nature of the machinery underlying the spatial restriction of Chs2p-myc to the mother-bud neck. Since Chs3p is already present throughout the cell cycle (Fig. 5; Ziman et al., 1996), the analogous experiment is not possible. Presumably, some form of cell cycle control modulates either Chs3p or its localization machinery, or both, to determine when Chs3p is retained at the bud site.

Chs2p-myc and Chs3p are predicted to be and behave

like integral membrane proteins (see Materials and Methods). Integral membrane proteins, if unrestrained, are expected to be uniformly distributed in the plasma membrane, according to the fluid-mosaic model as well as experiments measuring the diffusion of integral membrane proteins (Jacobson et al., 1987; Singer and Nicolson, 1972). Thus, the ability of Chs2p-myc and Chs3p to be retained to a specific region of the cell surface must depend on other elements. The 10-nm neck filaments (Byers, 1981; Longtine et al., 1996) represent a good candidate to provide a basis for neck localization. These filaments, which incorporate the *CDC3*, *10*, *11*, and *12* gene products (known collectively as the septins), form a ring under the plasma membrane in the neck region where Chs2p-myc and Chs3p are found. This filament ring appears at the time of bud emergence and persists until cytokinesis. Mutants in components of the neck filaments display a temperature-sensitive defect in cytokinesis (Pringle and Hartwell, 1981) and in chitin localization (as judged by delocalized Calcofluor staining; e.g., Flescher et al., 1993). These observations, in addition to the formation of septum-like structures at abnormal locations in these mutants (Slater et al., 1985), suggest that the neck filaments directly or indirectly localize Chs2p and Chs3p to the bud site and mother-bud neck. In support of this hypothesis, we have recently found that Chs3p staining is aberrant both in *cdc10* mutants and in mutants defective in septin-interacting gene products (*BNI4* and *CHS4*) (DeMarini, D., J.S. Chuang, and J. Pringle, manuscript in preparation).

Cabib et al. (1982) suggested that chitin synthases were uniformly distributed in the plasma membrane and that temporally and spatially restricted recruitment of a zymogen-activating factor resulted in regulated chitin deposition. Our observations of Chs2p-myc and Chs3p localization to regions of chitin synthesis at physiologically relevant times argue against localized activation as the primary mechanism regulating the timing and positioning of chitin deposition. Although we cannot generalize our model to include Chs1p, our data suggest that regulation of chitin deposition occurs by direct localization of the enzymes responsible for chitin synthesis.

Divergent Fates of Chs2p and Chs3p after Endocytosis

In pulse-chase experiments, we found that Chs2p-myc is an unstable protein and that its degradation depends on the proper functioning of the late secretory pathway, the early endocytic pathway, and the major vacuolar proteases (Fig. 6 *A*). These results, in combination with the observation that Chs2p-myc enters the ER (Fig. 1), suggest a basic pathway for the biogenesis of chitin synthase II. Chs2p enters the secretory pathway in the ER and travels through the Golgi complex, where it is packaged into transport vesicles and delivered to the plasma membrane in a manner indistinguishable from other cell surface proteins. The protein then becomes assembled into a ring structure, possibly organized by the septins at the nascent division septum. After cytokinesis, the enzyme is internalized and transported to the vacuole via an endosome. This picture of the biogenesis of Chs2p bears strong similarity to the biogenesis of the **a**-factor transporter, Ste6p (Berkower et al., 1994; Kölling and Hollenberg, 1994), except that Chs2p is subject to the additional complexity of regulated synthesis and localization.

The short half-life of Chs2p-myc is difficult to reconcile with the report of a significant internal pool of Chs2p-containing chitosomes at steady state (Leal-Morales et al., 1994). One possible explanation for this discrepancy is that internalization from the plasma membrane occurs so rapidly that a large proportion of the total Chs2p is in transit, either to or from the plasma membrane. It is also possible that Chs2p-myc and authentic Chs2p have different turnover rates. Another possibility stems from the different methods used to detect the protein. All previous studies of chitin synthase II relied on determination of enzymatic activity. The specific activity of chitin synthase II could vary among compartments and lead to an overestimate of the amount of internal vs cell surface–localized Chs2p. We did not detect Chs2p-myc in the chitosomal fraction isolated from lysed, Con A–coated spheroplasts (data not shown).

In contrast, a significant fraction of Chs3p is found in an internal pool of membranes, which are operationally defined as chitosomes (Fig. 7). Using differential centrifugation of metabolically labeled, Con A–coated spheroplasts, we found that ~30–50% of Chs3p resides in chitosomes. These membranes are efficiently separated from plasma membrane. Curiously, the distribution of newly synthesized Chs3p between chitosomes and the plasma membrane did not change markedly over a 90-min chase (Fig. 7) or even a 150-min chase (data not shown). This confusing observation is partially resolved by the demonstration that chitosomes are not present when endocytosis is blocked using an *end3-1* or *end4-1* mutant (Fig. 8 *B*). The effect of the *end* mutants on the distribution of Chs3p in the differential centrifugation assay may be an indirect effect of blocking endocytosis, e.g., by blocking the delivery of a factor involved in retaining Chs3p in the chitosome. However, the simplest interpretation of the *END3* and *END4* requirement is that chitosomes containing Chs3p are endocytically derived.

Taken together, our results on Chs3p suggest that it travels to and from the plasma membrane in parallel with Chs2p, but it remains in the endosome instead of traveling on to the vacuole for degradation. Thus, the chitosome may be a general endosome or a specific endosome-derived vesicle. Chs1p is also found in chitosomes in *END* but not *end4-1* strains (Ziman et al., 1996); thus, it may follow the same itinerary as Chs3p. Chitosomes could correspond to a specialized aspect of another secretory organelle. However, more extensive subcellular fractionation indicates that Chs1p and Chs3p-containing membranes do not correspond to the ER, Golgi, mitochondria, or vacuole (Ziman et al., 1996). In addition, the density of chitosomes does not match that of *sec1-1* secretory vesicles (Fig. 8 *A*), and biogenesis of invertase and carboxypeptidase Y are unaffected by *end4-1* (Raths et al., 1993).

In *S. cerevisiae*, many plasma membrane proteins (Ste2p, Ste3p, Ste6p, and Chs2p) that are known to undergo endocytosis are rapidly delivered to the vacuole (Berkower et al., 1994; Davis et al., 1993; Kölling and Hollenberg, 1994; Raths et al., 1993; Fig. 6 *A*). The metabolic stability of Chs3p (Fig. 6 *B*) is novel, considering that it appears to be subject to endocytosis. It is possible that internalized Chs3p is destined to travel to the vacuole, but that its tran-

sit time is somehow significantly delayed, possibly because of a positive endosome retention signal or the absence of a vacuole transport signal. Alternatively, we speculate that chitosomes may represent an endocytically derived compartment involved in the recycling of Chs3p. Recycling from the endosome/chitosome may rapidly localize Chs3p to the presumptive bud site at a time before polarization of the general secretory pathway is thought to occur. It is also possible that activation of CSIII enzyme activity at the division septum requires transit through the endosomal compartment.

By indirect immunofluorescence microscopy, we found that Chs3p localizes to the bud site in cells nearing bud emergence, in the neck of small-budded cells, and in some mitotic cells preparing for cell separation (Figs. 3 and 4). We have not detected neck localization in the period between bud emergence and cell separation. Since Chs3p is not rapidly degraded, it may disassemble and reassemble from the neck during the course of the cell cycle. Chs3p may be endocytosed into chitosomes after bud emergence, and some of it may be recycled in preparation for cell separation. An analogous process can also be envisioned for the interval between the completion of cell separation and the moments before bud emergence. During this period, Chs3p must be relocalized from the neck to the new bud site. At the same time, Chs3p is synthesized throughout the cell cycle. These overlapping events may explain why a shift in Chs3p distribution between the 10,000-*g* pellet and supernatant fractions was not seen in metabolically labeled cells.

What determines the distinct fates of Chs3p and Chs2p after endocytosis? Hicke and Riezman (1996) suggest that the ubiquitination state of plasma membrane proteins may serve to funnel internalized polypeptides through different branches of the endocytic pathway. Recycling of Chs3p and Chs1p, but not Chs2p, would provide an opportunity to identify sequence-specific sorting determinants and to search for proteins involved in this previously uncharacterized limb of the yeast secretory pathway.

We thank Michael Ziman for the integrated *PMA1HA* strain, and Christine Bulawa, James Haber, Randy Hampton, and the Thorner and Drubin labs for various plasmids, strains, and antibodies. We are grateful to the members of the Schekman lab for reagents, technical advice, and discussion, especially Michael Ziman for comments on the manuscript and for discussion throughout the course of this study.

This work was supported by a Howard Hughes Medical Institute predoctoral fellowship (to J.S. Chuang) and by the Howard Hughes Medical Institute (to R.W. Schekman).

Received for publication 29 May 1996 and in revised form 19 August 1996.

References

Ausubel, F.M., R. Brent, R.E. Kingston, D.D. Moore, J.G. Seidman, J.A. Smith, and K. Struhl. 1987–1995. Current Protocols in Molecular Biology. John Wiley & Sons, Inc., New York.

Baker, D., L. Hicke, M. Rexach, M. Schleyer, and R. Schekman. 1988. Reconstitution of *SEC* gene product-dependent intercompartmental protein transport. *Cell.* 54:335–344.

Bartnicki-Garcia, S. 1990. Role of vesicles in apical growth and a new mathematical model of hyphal morphogenesis. *In* Tip Growth in Plant and Fungal Cells. I.B. Heath, editor. Academic Press, Inc., San Diego, CA. 211–232.

Baum, P., J. Thorner, and L. Honig. 1978. Identification of tubulin from the yeast *Saccharomyces cerevisiae*. *Proc. Natl. Acad. Sci. USA.* 75:4962–4966.

Berkower, C., D. Loayza, and S. Michaelis. 1994. Metabolic instability and constitutive endocytosis of *STE6*, the a-factor transporter of *Saccharomyces cerevisiae*. *Mol. Biol. Cell.* 5:1185–1198.

Bulawa, C.E. 1992. *CSD2*, *CSD3*, and *CSD4*, genes required for chitin synthesis in *Saccharomyces cerevisiae*: the *CSD2* gene product is related to chitin synthases and to developmentally regulated proteins in *Rhizobium* species and *Xenopus laevis*. *Mol. Cell. Biol.* 12:1764–1776.

Bulawa, C.E. 1993. Genetics and molecular biology of chitin synthesis in fungi. *Annu. Rev. Microbiol.* 47:505–534.

Bulawa, C.E., and B.C. Osmond. 1990. Chitin synthase I and chitin synthase II are not required for chitin synthesis in vivo in *Saccharomyces cerevisiae*. *Proc. Natl. Acad. Sci. USA.* 87:7424–7428.

Bulawa, C.E., M. Slater, E. Cabib, J. Au-Young, A. Sburlati, W.L. Adair, Jr., and P.W. Robbins. 1986. The *S. cerevisiae* structural gene for chitin synthase is not required for chitin synthesis *in vivo*. *Cell.* 46:213–225.

Byers, B. 1981. Cytology of the yeast life cycle. *In* The Molecular Biology of the Yeast *Saccharomyces*: Life Cycle and Inheritance. J.N. Strathern, E.W. Jones, and J.R. Broach, editors. Cold Spring Harbor Laboratory, Cold Spring Harbor, NY. 59–96.

Cabib, E., R. Roberts, and B. Bowers. 1982. Synthesis of the yeast cell wall and its regulation. *Annu. Rev. Biochem.* 51:763–793.

Cabib, E., A. Sburlati, B. Bowers, and S.J. Silverman. 1989. Chitin synthase 1, an auxiliary enzyme for chitin synthesis in *Saccharomyces cerevisiae*. *J. Cell Biol.* 108:1665–1672.

Chant, J., and J.R. Pringle. 1995. Patterns of bud-site selection in the yeast *Saccharomyces cerevisiae*. *J. Cell Biol.* 129:751–765.

Chiang, H.-L., and R. Schekman. 1991. Regulated import and degradation of a cytosolic protein in the yeast vacuole. *Nature (Lond.).* 350:313–318.

Choi, W.-J., B. Santos, A. Durán, and E. Cabib. 1994*a*. Are yeast chitin synthases regulated at the transcriptional or the posttranslational level? *Mol. Cell. Biol.* 14:7685–7694.

Choi, W.-J., A. Sburlati, and E. Cabib. 1994*b*. Chitin synthase 3 from yeast has zymogenic properties that depend on both the *CAL1* and the *CAL3* genes. *Proc. Natl. Acad. Sci. USA.* 91:4727–4730.

Christianson, T.W., R.S. Sikorski, M. Dante, J.H. Shero, and P. Hieter. 1992. Multifunctional yeast high-copy-number shuttle vectors. *Gene (Amst.).* 110: 119–122.

Cid, V.J., A. Durán, F. del Rey, M.P. Snyder, C. Nombela, and M. Sanchez. 1995. Molecular basis of cell integrity and morphogenesis in *Saccharomyces cerevisiae*. *Microbiol. Rev.* 59:345–386.

Davis, N.G., J.L. Horecka, and G.F. Sprague, Jr. 1993. *Cis*- and *trans*-acting functions required for endocytosis of the yeast pheromone receptors. *J. Cell Biol.* 122:53–65.

Durán, A., and E. Cabib. 1978. Solubilization and partial purification of yeast chitin synthetase. Confirmation of the zymogenic nature of the enzyme. *J. Biol. Chem.* 253:4419–4425.

Evan, G.I., G.K. Lewis, G. Ramsay, and J.M. Bishop. 1985. Isolation of monoclonal antibodies specific for human c-*myc* proto-oncogene product. *Mol. Cell. Biol.* 5:3610–3616.

Feldheim, D., J. Rothblatt, and R. Schekman. 1992. Topology and functional domains of Sec63p, an endoplasmic reticulum membrane protein required for secretory protein translocation. *Mol. Cell. Biol.* 12:3288–3296.

Flescher, E.G., K. Madden, and M. Snyder. 1993. Components required for cytokinesis are important for bud site selection in yeast. *J. Cell Biol.* 122:373–386.

Flores Martinez, A., and J. Schwencke. 1988. Chitin synthetase activity is bound to chitosomes and to the plasma membrane in protoplasts of *Saccharomyces cerevisiae*. *Biochim. Biophys. Acta.* 946:328–336.

Harris, S.L., S. Na, X. Zhu, D. Seto-Young, D.S. Perlin, J.H. Teem, and J.E. Haber. 1994. Dominant lethal mutations in the plasma membrane H(+)-ATPase gene of *Saccharomyces cerevisiae*. *Proc. Natl. Acad. Sci. USA.* 91: 10531–10535.

Hemmings, B.A., G.S. Zubenko, A. Hasilik, and E.W. Jones. 1981. Mutant defective in processing of an enzyme located in the lysosome-like vacuole of *Saccharomyces cerevisiae*. *Proc. Natl. Acad. Sci. USA.* 78:435–439.

Hicke, L., and H. Riezman. 1996. Ubiquitination of a yeast plasma membrane receptor signals its ligand-stimulated endocytosis. *Cell.* 84:277–287.

Holcomb, C.L., W.J. Hansen, T. Etcheverry, and R. Schekman. 1988. Secretory vesicles externalize the major plasma membrane ATPase in yeast. *J. Cell Biol.* 106:641–648.

Jacobson, K., A. Ishihara, and R. Inman. 1987. Lateral diffusion of proteins in membranes. *Annu. Rev. Physiol.* 49:163–175.

Johnson, L.M., V.A. Bankaitis, and S.D. Emr. 1987. Distinct sequence determinants direct intracellular sorting and modification of a yeast vacuolar protease. *Cell.* 48:875–885.

Kölling, R., and C.P. Hollenberg. 1994. The ABC-transporter Ste6 accumulates in the plasma membrane in a ubiquitinated form in endocytosis mutants. *EMBO (Eur. Mol. Biol. Organ.) J.* 13:3261–3271.

Laemmli, U.K. 1970. Cleavage of structural proteins during the assembly of the head of bacteriophage T4. *Nature (Lond.).* 227:680–685.

Leal-Morales, C.A., C.E. Bracker, and S. Bartnicki-Garcia. 1988. Localization of chitin synthetase in cell-free homogenates of *Saccharomyces cerevisiae*: chitosomes and plasma membrane. *Proc. Natl. Acad. Sci. USA.* 85:8516–8520.

Leal-Morales, C.A., C.E. Bracker, and S. Bartnicki-Garcia. 1994. Subcellular localization, abundance and stability of chitin synthetases 1 and 2 from *Saccharomyces cerevisiae*. *Microbiology.* 140:2207–2216.

Longtine, M.S., D.J. DeMarini, M.L. Valencik, O.S. Al-Awar, H. Fares, C.D. Virgilio, and J.R. Pringle. 1996. The septins: roles in cytokinesis and other

processes. *Curr. Opin. Cell Biol.* 8:106–119.
Louvard, D., H. Reggio, and G. Warren. 1982. Antibodies to the Golgi complex and the rough endoplasmic reticulum. *J. Cell Biol.* 92:92–107.
Makarow, M. 1985. Endocytosis in *Saccharomyces cerevisiae*: internalization of enveloped viruses into spheroplasts. *EMBO (Eur. Mol. Biol. Organ.) J.* 4: 1855–1860.
Nakamoto, R.K., R. Rao, and C.W. Slayman. 1991. Expression of the yeast plasma membrane [H+]ATPase in secretory vesicles. A new strategy for directed mutagenesis. *J. Biol. Chem.* 266:7940–7949.
Novick, P., C. Field, and R. Schekman. 1980. Identification of 23 complementation groups required for post-translational events in the yeast secretory pathway. *Cell.* 21:205–215.
Orlean, P. 1987. Two chitin synthases in *Saccharomyces cerevisiae. J. Biol. Chem.* 262:5732–5739.
Pammer, M., P. Briza, A. Ellinger, T. Schuster, R. Stucka, H. Feldmann, and M. Breitenbach. 1992. *DIT101 (CSD2, CAL1)*, a cell cycle-regulated yeast gene required for synthesis of chitin in cell walls and chitosan in spore walls. *Yeast.* 8:1089–1099.
Pringle, J.R., and L.H. Hartwell. 1981. The *Saccharomyces cerevisiae* cell cycle. *In* The Molecular Biology of the Yeast Saccharomyces: Life Cycle and Inheritance. J.N. Strathern, E.W. Jones, and J.R. Broach, editors. Cold Spring Harbor Laboratory, Cold Spring Harbor, NY. 97–142.
Pryer, N.K., N.R. Salama, R. Schekman, and C.A. Kaiser. 1993. Cytosolic Sec13p complex is required for vesicle formation from the endoplasmic reticulum in vitro. *J. Cell Biol.* 120:865–875.
Raths, S., J. Rohrer, F. Crausaz, and H. Riezman. 1993. *end3* and *end4*: two mutants defective in receptor-mediated and fluid-phase endocytosis in *Saccharomyces cerevisiae. J. Cell Biol.* 120:55–65.
Roncero, C., M.H. Valdivieso, J.C. Ribas, and A. Durán. 1988. Isolation and characterization of *Saccharomyces cerevisiae* mutants resistant to Calcofluor white. *J. Bacteriol.* 170:1950–1954.
Sanz, P., E. Herrero, and R. Sentandreu. 1987. Secretory pattern of a major integral mannoprotein of the yeast cell wall. *Biochim. Biophys. Acta.* 924:193–203.
Sburlati, A., and E. Cabib. 1986. Chitin synthetase 2, a presumptive participant in septum formation in *Saccharomyces cerevisiae. J. Biol. Chem.* 261:15147–15152.
Shaw, J.A., P.C. Mol, B. Bowers, S.J. Silverman, M.H. Valdivieso, A. Durán, and E. Cabib. 1991. The function of chitin synthases 2 and 3 in the *Saccharomyces cerevisiae* cell cycle. *J. Cell Biol.* 114:111–123.
Sherman, F. 1991. Getting started with yeast. *Methods Enzymol.* 194:2–21.
Sherman, F., and J. Hicks. 1991. Micromanipulation and dissection of asci. *Methods Enzymol.* 194:21–37.
Sikorski, R.S., and P. Hieter. 1989. A system of shuttle vectors and yeast host strains designed for efficient manipulation of DNA in *Saccharomyces cerevisiae. Genetics.* 122:19–27.
Silverman, S.J. 1989. Similar and different domains of chitin synthases 1 and 2 of *S. cerevisiae*: two isozymes with distinct functions. *Yeast.* 5:459–467.
Silverman, S.J., A. Sburlati, M.L. Slater, and E. Cabib. 1988. Chitin synthase 2 is essential for septum formation and cell division in *Saccharomyces cerevisiae. Proc. Natl. Acad. Sci. USA.* 85:4735–4739
Singer, S.J., and G.L. Nicolson. 1972. The fluid mosaic model of the structure of cell membranes. *Science (Wash. DC).* 175:720–731.
Slater, M.L., B. Bowers, and E. Cabib. 1985. Formation of septum-like structures at locations remote from the budding sites in cytokinesis-defective mutants of *Saccharomyces cerevisiae. J. Bacteriol.* 162:763–767.
Smith, D.B., and K.S. Johnson. 1988. Single-step purification of polypeptides expressed in *Escherichia coli* as fusions with glutathione S-transferase. *Gene (Amst.).* 67:31–40.
Stevens, T., B. Esmon, and R. Schekman. 1982. Early stages in the yeast secretory pathway are required for transport of carboxypeptidase Y to the vacuole. *Cell.* 30:439–448.
Stirling, C.J., J. Rothblatt, M. Hosobuchi, R. Deshaies, and R. Schekman. 1992. Protein translocation mutants defective in the insertion of integral membrane proteins into the endoplasmic reticulum. *Mol. Biol. Cell.* 3:129–142.
Trimble, R.B., and F. Maley. 1977. Subunit structure of external invertase from *Saccharomyces cerevisiae. J. Biol. Chem.* 252:4409–4412.
Wilson, I.A., H.L. Niman, R.A. Houghten, A.R. Cherenson, M.L. Connolly, and R.A. Lerner. 1984. The structure of an antigenic determinant in a protein. *Cell.* 37:767–778.
Ziman, M., J.S. Chuang, and R.W. Schekman. 1996. Chs1p and Chs3p, two proteins involved in chitin synthesis, populate a compartment of the *Saccharomyces cerevisiae* endocytic pathway. *Mol. Biol. Cell.* In press.